

Chapter 7

Computer Tomography Phantom Applications

Paulo R. Costa

7.1 Historical Perspective

Computed tomography (CT) using X-rays was the first imaging modality used in Medicine associating computer processing with data obtained from patients' X-ray transmission. This innovative technique developed during the second half of the 1960s and available for clinical use in 1972 has brought a new vision about the contrast details of the patient's body. The architecture of CT machines associated with the wide-range sensitivity of the employed detectors becomes available a level of tissue differentiation not found before in any other imaging system. The powerful diagnostic capability, associated with the possibility of viewing slices of the body, recognized CT as one of the milestones on the development of clinical images in the last century [1].

Many visionary pioneers of the technical and conceptual development of CT scanners are reported in the literature, such as W. H. Oldendorf, D. E. Kuhl, R. Q. Edwards, and A. M. Cormack [2]. The introduction of this image modality to diagnostic Medicine was so accepted by the scientific community, that Sir Godfrey Hounsfield, who is recognized as the major contributor of the CT scanners development and who obtained the first patents of the CT apparatus in 1968 and 1972, was distinguished with the Nobel Prize in Physiology or Medicine in 1979. He shared this prize with the physicist Allan Cormack.

All these new possibilities of improving the diagnoses of known diseases and also recognizing new pathologies or early stages of pathological tissues were followed by the need of developing new methods for improving the image performance properties and the evaluation of doses in patients and staff. The drastic changes in the CT scanners architecture compared to other diagnostic X-ray machines presented as a new paradigm for Medical Physicists on determining dose

P. R. Costa (✉)

Department of Nuclear Physics, University of São Paulo, Rua do Matão, Travessa R, 187, São Paulo, SP 05508-090, Brazil

e-mail: pcosta@if.usp.br

characteristics thirty years ago. These architecture modifications included the change from plane-parallel to cylindrical geometry for example. The major challenge was in measurement for a cross section as opposed to a flat field. This new geometric aspect of the CT scanners, generating a narrow X-ray fan beam, which produced a radiation profile with axial symmetry inside the patient, required been adequately quantified by a dosimetric parameter or function unknown until that time. Later, a “dose index” for CT applications was introduced to cover this need.

After the first developments of quality assurance and dose assessment of early-generation CT scanners, it was clear for the professionals working on technical aspects of measurements adequacy for improving the safety of patients and the assurance of high image qualities that the evolution of the systems available in the market will be very fast [3]. The engineering teams of the CT vendors are constantly searching for better spatial resolution, thinner slices and faster image acquisitions and reconstruction algorithms. However, these factors also represent constant need for new measurement techniques and phantoms, corresponding to the crescent changes on the CT equipment capabilities. Since the end of the last century, Medical Physicists and Radiologists saw the emergence of new CT technologies, such as multi-slice, current-modulated, half-second rotation, dual-energy, dedicated breast, and 4D cone beam. Each one of them presents new diagnostic capabilities, but individually requires new studies in quality control and dosimetry. The development of phantoms followed the same process, and it shows to be of major importance on the qualification of the CT scanners in order to balance patient safety and diagnostic capabilities. During this time, radiation doses [3] and dose reduction techniques [4] have been a constant concern for the medical physicists and other professional involved with this kind of imaging technique.

Recently, an impressive growth has been observed in the use of new imaging technologies employing ionizing radiation, in special CT machines [5, 6]. A study conducted by Fazel et al. [7] demonstrated that around 75 % of the dose in the North American population during the years between of 2005 and 2007 was related to CT and Nuclear Medicine procedures in this period. However, these two techniques represented only 21 % of the imaging procedures conducted in that population. These numbers alerted the community for the need of systematic dose assessment in CT examinations and increasing the investments in education in all levels associated with the radiologic image chain (radiologist,technologist, physicists, nurses, engineers, administrators, etc.) to recognize the correct risks associated with these clinical protocols [8, 9].

7.2 Acceptance and Quality Control Testing

7.2.1 Phantoms for Accessing Dosimetry

During the second half of the 1970s, many papers appeared in the literature describing methodologies and devices for the dosimetric characterization of CT systems [10, 11]. These methods, however, were just organized in a consistent

manner with the introduction of the CT dose index (CTDI) by Shope et al. [12]. This index, which was (and is) frequently confounded with patient dose [13], formed the mathematical, conceptual, and experimental base for the dosimetric characterization of CT machines and protocols [14]. Nowadays, there are substantial improvements of the original CTDI definitions. These definitions can be found in the literature [15], and deeply exploring their concepts is out of the context of the present work. Moreover, with the recent changes on the architecture of the CT machines, these CT metrics are in progress of adaptation to be used (or not) when evaluating doses to wide-beam CT systems. Very comprehensive texts are available discussing the recent developments in CT dosimetry [16].

The CTDI definition considers the dose profile as composed of a superposition of a primary dose distribution, related to the portion of the X-ray beam modulated by the pre-patient collimator, which is used to produce the image, and a scatter profile, originated the interaction of the primary beam with a phantom material. The standardized phantom material chosen to be used in CTDI measurements was the polymethyl methacrylate (PMMA). The International Electrotechnical Commission adopted this CTDI measuring method for comply its dosimetric requirements for CT equipment [17].

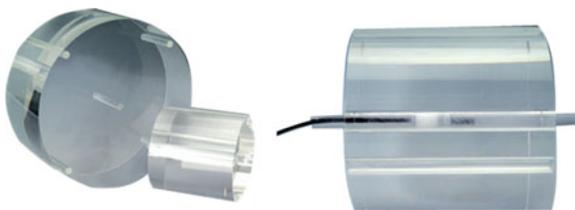
Dose measurements can be performed in two ways: computing the CT dose profiles or integrating the average signal with an ionizing chamber [18], [19]. The dose profile methods were traditionally performed by using TLD's aligned in rows and positioned inside the dosimetric phantom [20]. More recently, this time-consuming method has been substituted by the use of OSL strips [21–23], Gafchromic films [24] or MOSFET detectors [25]. Using these kinds of approaches, it is possible to recognize not only the dosimetric properties, but also the geometric properties of the radiation profile, and to compare it with the sensitive CT profiles for different collimations [26].

The methodologies using position-sensitive devices above described are not practical for routine dosimetry of CT scanners. In these cases, the use of pencil-shaped ion chambers is preferred. The use of ion chambers specific for CT was introduced by Suzuki and Suzuki [27] and it is widely applied today. Similar to the re-evaluation of the applications of CTDI, considering the new scanner designs, the use of these pencil chambers has been discussed in the scientific community [28–30]. One of the proposed alternatives is the use of a farmer-type detector for dose evaluation purposes of wide-beam scanners [31].

Anyway, independently of the dosimetry methodology chosen, the traditional phantom design is composed of cylindrical blocks of massive PMMA with standardized diameters (16 and 32 cm) representing parts of the body (head or trunk/abdomen) for adult or pediatric dose assessment (Fig. 7.1). These plastic blocks have holes with diameters adequate for inserting the pencil ion chambers, the position-sensitive dosimeters, or farmer-type chambers [32].

The experience of using these cylindrical blocks, associated with the searching for more detailed dosimetric information, conducted the industry to develop some more sophisticated CTDI phantoms. Two examples of these different solutions are shown in Figs. 7.2 and 7.3. Figure 7.2 presents a stack of PMMA blocks forming a

Fig. 7.1 Head and body CT dosimetric phantom manufactured by Radcal Corporation. The phantoms are composed of cylindrical massive blocs of PMMA containing holes dimensioned for the exact introduction of pencil ion chambers



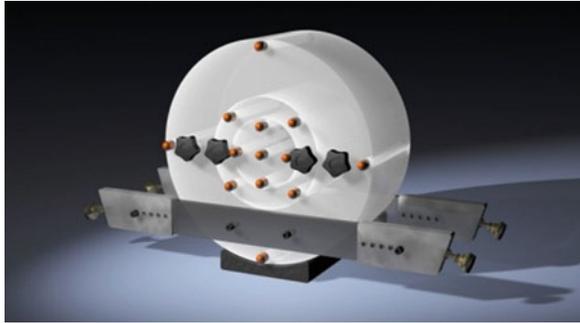
system which represents a human head. This phantom was designed for cone beam CT (CBCT) dose evaluations and can also be used for CT dose evaluations with TLD's, ionization chambers or Gafchromic films. On the other hand, Fig. 7.3 shows a new development of dosimetric phantom composed of nesting PMMA disks with standardized diameters for evaluating CTDI for pediatric and adult protocols. The phantom can be coupled to a support, which suspends the device over the equipment couch and aligns it along the central axis of the imaging system. It enables the use of the phantom in helical mode of operation of the CT equipment.

An important use of different size and shape acrylic phantoms for pediatric dose investigations in CT was conducted by Siegel et al. [33]. The study analyzed the dosimetric response of a multi-detector CT scanner when parameters such as applied voltage, AEC, and size and shape of the phantoms are associated with image noise and contrast. They found that the measured doses in an 8-cm-diameter phantom are superior to 50 and 100 % for applied voltages of 80 and 140 kV, respectively, when compared to the doses measured using a 32-cm-diameter phantom adopting a protocol-defined tube current value. However, when the tube current was adapted to the phantom size, the dose reduction for the 8-cm-diameter

Fig. 7.2 SedentexCT dose phantom composed of a stack of PMMA blocks forming a system which represents a human head (www.leadstestobjects.com)



Fig. 7.3 Dosimetric phantom composed of nesting PMMA disks with standardized diameters for evaluating CTDI for pediatric and adult protocols (www.cirsinc.com)



phantom was about 80 %. They also found that the reduction in the applied voltage can increase the image noise significantly. This kind of study using different size and shape of geometric phantoms generated many initiatives on optimizing pediatric CT imaging protocols [34].

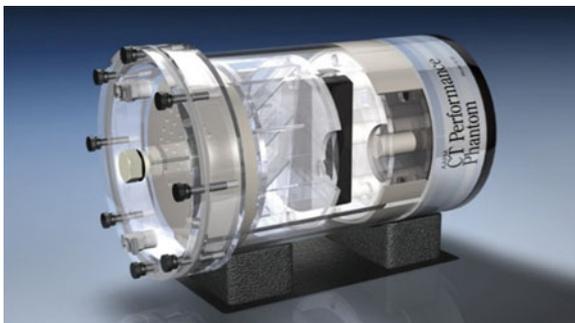
7.2.2 Phantoms for Accessing Image Quality

After the introduction of the commercial CT scanners by EMI in the early 1970s, the scientific community started to evaluate the capabilities and limitations of that new imaging device [35]. However, the previously known image quality evaluation techniques were not adapted to the geometric characteristics of the CT scanners neither to their physical and architectonic properties, such as voltage and current range and gantry geometry. This situation resulted in proposals for geometric apparatus intending to quantify the main image properties of the CT images, such as spatial resolution in low- and high-contrast background, image noise, slice thickness, and also some kind of artifacts (motion, beam hardening, uniformity).

A few years after the popularization of the CT device in the clinical environment, Edwin McCullough, from Mayo Clinic, published two papers showing the applications of a PMMA test object for the evaluation of the image quality of commercial scanners [36, 37]. The McCullough and colleagues' ideas have contributed to the AAPM Task Force on CT Scanner Phantoms, and their progresses were adopted on the first guide for quality control and dosimetry in CT published by AAPM [38], and which based the development of many posterior quality control programs [39]. The AAPM CT test phantom (Fig. 7.4) also included an insert for TLD measurements of the dose profile and alignment. This phantom was widely used around the world for at least 20 years for establishing quality control and acceptance testing programs for CT scanners.

The AAPM CT quality control phantom includes many interesting inserts for performance evaluation of the CT scanners in terms of its image quality, but it is

Fig. 7.4 CIRS Model 610 phantom which complies with the recommendations of the AAPM for a CT performance phantom [38]. The phantom measures ten distinct CT performance parameters



inconvenient because of the need to be filled with water. In order to develop more practical methods for evaluating image quality in CT, several solid phantoms were developed for this purpose. One of the most familiar solid quality assurance CT phantom was proposed based on the works of Goodenough and collaborators [40, 41] using a tissue-equivalent epoxy resin developed by White [42]. This phantom was improved during the last decades and received specific inserts and accessories for taking into account the different requirements for image quality evaluation resulting from technological development of the CT scanners (Fig. 7.5). The phantom is made from solid-cast materials, eliminating material absorption of water and leaks associated with water bath phantoms, as well as problems related to varied water sources.

Other kind of modular phantom for image quality assessment purpose is presented in Fig. 7.6. This phantom was developed in a modular design and in the body of the phantom are holes for inserting small disks which provide specific information about image quality parameters, such as spatial and contrast resolution, pixel intensity, beam hardening, geometric distortion, uniformity and noise.

There are many other phantoms for CT image quality which can be found in the specialized market. This text has not the intention to provide comprehensive information for all available phantom models neither to exclude any commercial product. The phantom option many times depends on the basic QA protocol

Fig. 7.5 Catphan[®] quality image solid phantom manufactured by The Phantom Laboratories [43]

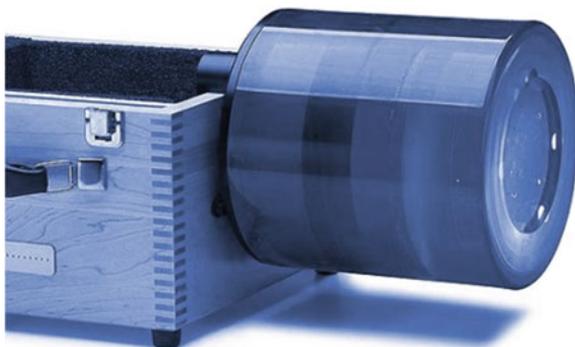


Fig. 7.6 Phantom developed in a modular design with holes for inserting small discs which provide image quality information (www.leedstestobjects.com)



adopted by the imaging facility [44, 45]. Other important kinds of solid phantom to be considered are related to accreditation programs for CT devices. These phantoms will receive a special topic in this chapter.

7.3 Use of Phantoms in the Accreditation Process

The definition of accurate criteria for quality assessment in CT systems was very closely connected to the development of specific phantoms. The AAPM Task Group number 2 was focused on acceptance tests of CT machines, and its report 39 [20] recommended the combined use of commercial phantoms to some generic objects designed specifically for the compliance to the document.

In 2000, the European Community expanded the concept of Quality Criteria Guidelines existing for other imaging modalities for CT [46]. In this document, guidance is adopted for establishing quality criteria and equipment performance associated with patient doses. The purpose was to provide an operational framework for radiation protection, correlating adequate technical parameters for generating images with good quality and the radiation safety of the patients.

The more contemporary and sophisticated concepts of quality assessment in medical imaging are included on the accreditation programs. The American College of Radiology (ACR) introduced a CT accreditation program ten years ago. The program involves the submission of information regarding the clinical protocols adopted in the facility, dose measurements, and the performance evaluation using clinical and phantom images [47]. The phantom designed for the image quality assessment required for the ACR accreditation program has the capability of providing information of positioning accuracy, accuracy of the CT No., slice

Fig. 7.7 ACR CT Phantom manufactured by Gammex, Inc. The phantom is designed to be an integral part of the American College of Radiology CT Accreditation Program



width, low contrast resolution, spatial resolution in high-contrast, CT number uniformity, and image noise [48].

The ACR CT accreditation phantom (Fig. 7.7) is composed of four modules constructed by water-equivalent material. The diameter of the phantom is 20 cm, and each module has 4 cm depth. They also have inserts which produces structures on the CT images for assessment of the characteristic quality parameters above described.

The ACR accreditation process also requires the submission of CTDI measurements. The context of these measurements are the same used in regular QC procedures, considering the adequate care to the alignment of the measuring setup. The phantoms used are the 16- and 32-cm-diameter PMMA blocks mentioned above, and the applicant must submit measurements resulting of the application of protocols for adults (head and abdomen) and pediatric (abdomen) examinations.

7.4 Anthropomorphic Phantoms for CT Applications

Anthropomorphic phantoms were introduced in radiation protection in Medicine with the aim of mimicking human tissue radiation absorption properties, and also its average anatomical characteristics such as electron density and effective atomic number variations. Alderson et al. [49] introduced the concepts of tissue-equivalent material [50] associated with a human-shaped phantom for applications in radiation therapy treatment plans (see Chap. 4). These dosimetric phantoms were constructed using a real human skeleton embedded in a material which mimics the human soft tissue. They also included a low density tissue for molding the shape of the lungs. This was called the “Alderson Phantom” and it is widely applied in diagnostic imaging dosimetry for varied applications [51], usually associated with the insertion of film or thermoluminescent dosimeters [52]. This kind of realistic phantom

has shown to be very useful for CT dosimetry since the beginning of the dose investigations of this technique [53].

The idea of using tissue-equivalent materials for CT evaluation purposes has been in place for at least 30 years [54]. Recently, anthropomorphic phantoms have been applied for dose estimation in CT in a wide assortment of applications using different kind of radiation detectors. The phantom exemplified in Fig. 7.8 is composed of a proprietary urethane formulation for mimic human soft tissue. This material has an effective atomic number and mass density which simulates muscle tissue with randomly distributed fat. The phantom also has lung material with the same effective atomic number as the soft tissue material, but with a density which simulates lungs in a median respiratory state, and a natural human skeleton [55].

Many authors have dedicated special attention to the high doses usually resulting from applying angiographic CT in Cardiology. For example, Nikolic et al. [56] associated a commercial phantom to semiconductor field-effect detectors in order to investigate the consequences of voltage and heart beats frequency on the absorption of radiation dose in radiosensitive organs. In 2006, Hurwitz et al. [57] published a study regarding female breast doses using a gender-specific phantom. A similar approach was adopted by Litmanovich et al. [58] on studying the effects of scanner parameters on breast, lung, and pelvic organs employing a female phantom. TLD evaluation using anthropomorphic phantoms and ionization chamber measurements with PMMA cylindrical phantoms can also be related to Monte Carlo simulations, providing very reliable information regarding 3D dose distributions resulted from CT imaging procedures [59]. These authors have considered important aspects of the protocols such as patient size, the use of tube current modulation, and the scanner architecture.

Researchers have also been motivated to use anthropomorphic phantoms for investigation of the sex-dependent tissue-weighting factors adopted by



Fig. 7.8 The RANDO[®] phantom manufactured by The Phantom Laboratory. The phantom is composed of a proprietary urethane formulation for mimicking human soft tissue [55]

International Commission on Radiation Protection publication 103 [60]. Monte Carlo simulations have been widely used for this purpose and also for evaluating age-specific dose characteristics.

One of the first results for the estimation of effective dose for pediatric CT examinations with Monte Carlo simulations was published by Huda et al. [61]. The authors adopted simple mathematical anthropomorphic age-specific phantoms for obtaining body region factors correlating effective doses and energy imparted during CT procedures. A more recent Monte Carlo simulation approach to this problem was published by Deak et al. [62] relating these factors to previously measured dose-length product (DLP) values. Different practical situations were investigated by these authors: four scanner voltages, five patient sizes/ages, and five body regions with dosimetric interest. Using these input parameters and the Oak Ridge National Laboratory phantom series [63], they calculated a series of conversion factors for calculation of the effective dose from measured values of DLP. They also compared their results when considering the recommendation of two different ICRP publications (60 and 103).

A complementary size-/age-specific Monte Carlo-based dosimetric approach was developed by Melo Lima et al. [64]. In this study, age- and posture-specific children mathematical phantoms were used. These phantoms are based on the technique developed by Kramer et al. [65] for adult male and female phantoms called MASH and FASH obtained from anatomical atlas using 3D modeling software [66]. Recently, these authors published results of skeleton dosimetry based on micro-CT images using the same anatomical models [67].

In general, in the last decades, the scientific community has promoted many efforts to consolidate special care in radiation protection in pediatric radiology. This special attention is clearly demonstrated by the Image Gently[®] campaign, an alliance focusing radiation safety in pediatric imaging, started in 2006 by the US Society of Pediatric Radiology, but which also involves many different segments of the society around the world. Dose evaluation and optimization in CT pediatric procedures have been adopted as one of the most studied issues of radiation dosimetry in the recent years [68], and the use of age-specific anthropomorphic phantoms has been adopted by the researchers for non-invasive determination of dose characteristics for these special procedures. A few years ago, stakeholders involved in this subject were stimulated by the Image Gently Alliance to work in partnership and define a vendor summit to bring the dose optimization in pediatric CT inside the clinical routine [69].

In the beginning of the last decade, a group from University of Texas elaborated strategies for conducting adequately CT procedures in pediatric patients [70]. They used commercial phantoms which simulate body proportions of children of 1, 5, and 10 years old and also an adult phantom and compared their superficial dose measurements with CTDI data, using the noise as an image quality parameter. They found that dose reductions in the range of 60–90 % are possible when the technical parameters are adequate to age-/size-specific patients. More recently, pediatric anthropomorphic phantoms were used in order to estimate organ doses

delivered by multi-detector CT scanners using or not an automatic exposure control system [71].

The popularization of the multi-detector CT scanners around the world brings many diagnostic advantages to the clinical area, but also resulted in a gap of knowledge about the dosimetric properties of these large-field CT machines and their effects in the human health. In 2007, Birnbaum et al. [72, 73] published a study using a customized abdominal anthropomorphic phantom constructed with tissue-equivalent materials and presented a cross-comparison of models and manufactures of CT machines. Their approaches were focused on the soft tissue contrast differentiation among commercial machines.

Other very important topics in terms of radiation protection that must be considered are doses in the fetus when a pregnant patient is submitted to CT procedures, especially in the cases of abdominal examinations. In such cases, careful considerations relating the fetal dose estimation and the associated risk must be conducted, taking into account the pregnancy stage and the characteristics of the CT procedure. These kinds of investigation are generally conducted using anthropomorphic phantoms.

Wagner et al. [74] presented a guide for orientation of the medical community when conducting X-ray examination on pregnant women. In a posterior publication, Wagner et al. [75] have treated the case of conceptus doses considering CT examinations. Osei and Falkner [76] studied fetal doses in general radiologic examinations and proposed an algorithm for estimating the fetal dose [77] and the associated risks [78]. Their studies were based on Monte Carlo simulations. Recently, CT evaluation doses were incorporated to the method [79] as well as the risk estimation [80].

Empirical CT fetal dose studies using anthropomorphic phantoms were introduced by Felmler et al. in 1990 [81] and more recently by Dietrich et al. [82], Hurwitz et al. [83], Jaffe et al. [84, 85], and finally by Gilet et al. [86]. These last authors used an anthropomorphic phantom and TLD's for determining fetal doses resulting from pulmonary CT angiograms and abdominal and pelvic CT procedures considering 4-, 16-, and 64-slice multi-detector scanners. Early pregnancy and gestational ages of 10, 18, and 38 weeks were considered. An Alderson anthropomorphic phantom was modified by adding soft tissue attenuation-equivalent material to simulate the different pregnancy stages considered in the study.

Other types of anthropomorphic phantoms are constructed using tissue-equivalent materials mimicking specific parts of the body. The differences on the radiation attenuation resulting from the anatomy of the body can also be evaluated using PMMA slabs filled with water. These kinds of devices and also a group of semi-anthropomorphic phantom were very recently used by Wang et al. [87]. These specific anthropomorphic or semi-anthropomorphic phantoms, filled with water or composed of tissue-equivalent materials, are practical and useful for investigating very specific dosimetric properties of the CT procedures or defined parts of the body. Birnbaum et al. [72, 73] have also developed specific tissue-equivalent materials for testing attenuation properties of CT protocols taking into

account different situations (scanner type, convolution kernel, and tube current). Tissue-equivalent materials were also developed by Peng [88] for a specific population.

7.5 Phantoms for Investigation of Specific Imaging and Dosimetry Issues

Currently, the CT becomes a general nomenclature for an image modality which has been reconfigured in more specialized sub-modalities. Specific system designs, image processing methods, accessories, or hardware improvements provide clinical capabilities and dose reduction which were not common in the CT facilities years ago. Examples of this new CT specialized and sub-modalities are the systems designed to cardiac or breast imaging, respectively, providing fast data collection and high contrast, with doses as low as possible. Dual-energy CT devices are other example of these new technologies.

The technological advances in CT systems are followed by the need of investigating specific characteristics in terms of image quality or dosimetry. Frequently, these investigations require the development and validation of phantoms to be applied focusing some specific capability of the CT device or the amount or radiation impinging the patient for make this clinical information available [89].

The effectiveness of current modulation on providing dose reduction when the radiation output is changed according to the patient body attenuation is one of the more intensively investigated property of modern CT systems. This operational characteristic is patient specific but must be implemented following an acceptable image noise standard, in order to produce images clinically acceptable. Since the current modulation depends on the attenuation, anthropomorphic, semi-anthropomorphic, or cylindrical dosimetry phantoms can be used for quantify the dose optimization resulting from its use. Duan et al. [90] used such phantoms for determining surface dose reduction using organ-based current modulation protocols. Incorrect operations of these systems were also investigated by Matsubara et al. [91] using commercial elliptical phantoms when the centralization of the patient is inappropriate.

Specifically designed phantoms are also proposed for determining the correct operation of current modulation systems. This approach was originally introduced by Kalender et al. [92] evaluating one of the first commercial equipment's providing current modulation option. The ImPACT program proposes the use of a conical PMMA block (Fig. 7.9) for testing the response of the modulation system when the patient size changes on the z-direction [93].

Dual-source CT equipment was introduced in the middle of the last decade. They offer an important contribution to cardiac CT images, providing better temporal resolution during ECG-controlled clinical procedures [94]. McCollough et al. [95] adopted the methodology described in IEC standard 60601-2-44 [17] for

Fig. 7.9 Conical PMMA block for testing AEC response of the system when the patient size changes on the z-direction [96]



determining the dose performance of a dual-source 64-slice system. This method adopts the widely used PMMA blocks with different diameters for measuring dose indexes.

The involuntary motions of the human body have also been focused by researchers looking for quality or dosimetric evaluations of CT protocols. One of the first studies considering these involuntary characteristics was conducted by Morehouse [97]. More recently, results of investigations which contribute to the development of flow and/or motion phantoms can be found in the literature [98, 99]. These devices can be designed for a domestic evaluation, or they can be produced focusing future validation and commercial use [100].

7.6 Perspectives on Phantom Developments for Image Quality and Dosimetry in CT

The development of phantoms occurred since the first generations of the CT machines until recently introduced large beam equipment was strongly related to the geometrical aspects of the systems, and to their image capabilities. Additionally, the development of CT technologies implicated the evolution of dose indicators and metrics, which consequently has influenced the design and validation of devices and measurement techniques for describing the dose aspects related to these imaging procedures. In the future, this compromise between technological developments and phantom designs will be maintained and, probably, consolidated.

An example of the strong relationship between new imaging technologies and the phantom design evolution is the assessment of image quality of dedicated breast CT equipment. In this kind of image, the sensitivity profile is one of the most important parameters to be evaluated, since it is related to the efficiency of the equipment on producing an image using the amount of radiation impinging in

considered slice of the patient body. Additionally, the breast tissue presents specific characteristic which must be taken into account in order to reproduce the response of the system when this kind of image is performed. These technical and anatomical constrains were recently considered by Nosratieh et al. [101]. These authors did an adaptation on a commercial adipose tissue phantom introducing circular brass disks into the phantom slabs, which were used for the slice-sensitive profile (SSP) evaluation. This example shows how new phantoms can be creatively designed in the future adopting as basis existing materials and simple, but effective, adaptations.

Other correlations that will probably influence the creation of new phantoms are the consideration of patient motion. Many efforts have been made for allocating the body involuntary motion as one of the variables to be considered on phantom designs. These considerations usually implicate on the introduction of mechanically induced motion with amplitude and frequency which mimic the natural motion of some part of the body. These kinds of considerations are especially important if the image sequence has the purpose to be used on cancer treatment procedures. Szegedi et al. [102] emphasizes the importance of the use of the four-dimensional CT as a tool for characterizing patient-specific organ/tumor motion. For this purpose, the authors developed a deformable liver phantom which can be moved simulating the displacement of this organ with the patient breath. The simulation of this movement is performed by a piston coupled to the liver phantom.

These works above mentioned are just two examples of many which can be found in the literature. The extension of number of published works reinforces the perspective of the future development of phantoms adapted of specifically designed for attending the need of image quality or dosimetric information on CT field. This is a very exciting research area which is following very closely the strong developments of new CT technologies.

A more specific development is been working by the AAPM Task Group 200. This TG is working out on the elaboration of practical measuring methods for accounting the metrics introduced at AAPM report 111 [16]. Their proposed measuring solution considers the use of a larger phantom to capture the scatter tails of the radiation profile and changes on the dosimetric CT protocols, considering not only with single axial scans but also with helical scans [103]. The proposed phantom is been designed as a cylinder constructed on high density polyethylene 30 cm in diameter and 60 cm in length, including some inserts and holes for the introduction of radiation detectors. This phantom is in validation phase and, after been incorporated as a regular-use tool for dosimetric assessment in CT scanners, will probably be a major change in the CT phantoms scenario used until today.

References

1. Keevil, S. F. (2011). Physics and medicine: A historical perspective. *Lancet*, 379, 1517–1524. (Published Online April 18 2012).
2. Webb, S. (1990). *From the watching of shadows—The origins of radiological tomography*. Bristol: Adam Hilger, ed.
3. Rothenberg, L. N., & Pentlow, K. S. (1992). Radiation dose in CT. *Radiographics*, 12, 1225–1243.
4. McCollough, C. H., Bruesewitz, M. R., & Kofler, J. M, Jr. (2006). CT dose reduction and dose management tools: Overview of available options. *RadioGraphics*, 26, 503–512.
5. Brenner, D. J., & Hall, E. J. (2007). Computed tomography: An increasing source of radiation exposure. *New England Journal of Medicine*, 357, 2277–2284.
6. Nickoloff, E. L., & Alderson, P. O. (2001). Radiation exposures to patients from CT: Reality, public perception, and policy. *American Journal of Roentgenology*, 177, 285–287.
7. Fazel, R., Krumholz, H. M., Wang, Y., Ross, J. S., Chen, J., Ting, H. H., Shah, N. D., Nasir, K., Einstein, A. J., and Nallamothu, B.K. (2009). Exposure to Low-Dose Ionizing Radiation from Medical Imaging Procedures. *N Engl J Med*, 361, 849–857. doi:10.1056/NEJMoa0901249.
8. Fayngersh, V., & Passero, M. (2009). Estimating radiation risk from computed tomography scanning. *Lung*, 187, 143–148.
9. Freudenberg, L. S., & Beyer, T. (2011). Subjective perception of radiation risk. *Journal of Nuclear Medicine*, 52(Suppl 2), 29S–35S.
10. International Commission on Radiological Protection. (2007b). *Managing patient dose in multi-detector computed tomography (MDCT)*. ICRP Publication 102. Annals of the ICRP 37(1). Elsevier ed.
11. Thomadsen, B. R., Paliwal, B. R., Laursen, J. F., Filamor, C. O., & van de Geijn, P. (1983). Some phantom designs for radiation dosimetry and CT applications. *Medical Physics*, 10, 886–888.
12. Shope, T. B., Gagne, R. M., and Johnson, G. C. (1981). A method for describing the doses delivered by transmission x-ray computed tomography. *Med Phys*, 8(4), 488–495.
13. McCollough, C. H., Leng, S., Yu, L., Cody, D. D., Boone, J. M., & McNitt-Gray, M. F. (2011). CT Dose Index and patient dose: They are not the same thing. *Radiology*, 259, 311–316.
14. McCullough, E. C., & Payne, J. T. (1978). Patient dosage in computed tomography. *Radiology*, 129, 457–463.
15. American Association of Physicists in Medicine. (2008). The measurement, reporting and management of radiation dose in CT. Report No. 96 of AAPM Task Group 23, Available in <http://www.aapm.org/pubs/reports/>.
16. American Association of Physicists in Medicine (2010). Comprehensive methodology for the evaluation of radiation dose in x-ray computed tomography. Report No. 111 of AAPM Task Group 111. Available in <http://www.aapm.org/pubs/reports/>.
17. International Electrotechnical Commission. (2009). *Medical electrical equipment: Part 2–44—Particular requirements for the safety of x-ray equipment for computed tomography*. Publication no. 60601-2-44. Ed. 3.: International Electrotechnical Commission, 1–36. Geneva, Switzerland.
18. Furlow, B. (2010). Radiation dose in computed tomography. *Radiologic Technology*, 81, 437–450.
19. Knox, H. H., & Gagne, R. M. (1996). Alternative methods of obtaining the computed tomography dose index. *Health Physics*, 71, 219–224.
20. Lin, P.-J. P., Beck, T.J., Borrás, C., Cohen, G., Jucius, R.A., Kriz, R.J., Nickoloff, E.L., Rothenberg, L.N., Strauss, K.J., Villafana, T. (1993). Specification and acceptance testing of computed tomography scanners. Report No. 39 of AAPM Task Group 2. Available in <http://www.aapm.org/pubs/reports/>.

21. Lavoie, L., Ghita, M., Brateman, L., & Arreola, M. (2011). Characterization of a commercially-available, optically-stimulated luminescent dosimetry system for use in computed tomography. *Health Phy*, *101*, 299–310.
22. Vrieze, T. J., Sturchio, G. M., & McCollough, C. H. (2012). Precision and accuracy of a commercially available CT optically stimulated luminescent dosimetry system for the measurement of CT dose index. *Medical Physics*, *39*, 6580–6584.
23. Yukihara, E. G., Ruan, C., Gasparian, P. B. R., Clouse, W. J., Kalavagunta, C., & Ahmad, S. (2009). An optically stimulated luminescence system to measure dose profiles in x-ray computed tomography. *Physics in Medicine & Biology*, *54*, 6337–6352.
24. Gorny, K. R., Leitzen, S. L., Bruesewitz, M. R., Kofler, J. M., Hangiandreou, N. J., & McCollough, C. H. (2005). The calibration of experimental self-developing Gafchromic® HXR film for the measurement of radiation dose in computed tomography. *Medical Physics*, *32*, 1010–1016.
25. Mukundan, S., Wang P. I., Frush, D. P., Yoshizumi, T., Marcus, J., Kloeblen, E., and Moore, M. (2007). MOSFET Dosimetry for Radiation Dose Assessment of Bismuth Shielding of the Eye in Children. *American Journal of Roentgenology*.*188*:1648–1650.
26. Gagne, R. M. (1989). Geometrical aspects of computed tomography: Sensitivity profile and exposure profile. *Medical Physics*, *16*, 29–37.
27. Suzuki, A., & Suzuki, M. N. (1978). Use of a pencil-shaped ionization chamber for measurement of exposure resulting from a computed tomography scan. *Medical Physics*, *5*, 536–539.
28. Boone, J. M. (2007). The trouble with CTD100. *Medical Physics*, *34*, 1364–1371.
29. Brenner, D. J., & McCollough, C. H. (2006). It is time to retire the computed tomography dose index (CTDI) for CT quality assurance and dose optimization. *Medical Physics*, *33*, 1189–1191.
30. Dixon, R. L. (2003). A new look at CT dose measurement: Beyond CTDI. *Medical Physics*, *30*, 1272–1280.
31. Dixon, R. L. et al. (2010). The future of CT dosimetry—Comprehensive methodology for the evaluation of radiation dose in x-ray computed tomography. Report of AAPM Task Group III.
32. International Atomic Energy Agency (IAEA). (2007). Dosimetry in diagnostic radiology: An international code of practice. Technical Reports Series No. 457 (IAEA).
33. Siegel, M. J., Schmidt, B., Bradley, D., Suess, C., & Hildebolt, C. (2004). Radiation dose and image quality in pediatric CT: Effect of technical factors and phantom size and shape. *Radiology*, *233*, 515–5221.
34. Ngaile, J. E., Msaki, P., & Kazema, R. (2012). Patient-size-dependent radiation dose optimisation technique for abdominal CT examinations. *Radiation Protection Dosimetry*, *148*, 189–201.
35. McCullough, E. C. (1980). Specifying and evaluating the performance of computed tomography (CT) scanners. *Medical Physics*, *7*, 291–296.
36. McCullough, E. C., Raker, H. I., Houser, O. W., & Reese, D. F. (1974). An evaluation of the quantitative and radiation features of a scanning x-ray transverse axial tomography: the EMI scanner. *Radiology*, *111*, 709–715.
37. McCullough, E. C., Payne, J. T., Baker, H. L., Hattery, R. R., Sheedv, P. P., Stephens, D. S., et al. (1976). Performance evaluation and quality assurance of computed tomography (CT) equipment with illustrative data for ACTA, delta and EMI scanners. *Radiology*, *120*, 173–188.
38. Judy P. F., Balter, S., Bassano, D., McCullough, E.C., Payne, J.T. & Rothenberg, L. (1977). *Phantoms for performance evaluation and quality assurance of CT scanners*. AAPM report nr. 1. American Association of Physicists in Medicine, Chicago.
39. Bellon, E. M., Miraldi, F. D., & Wiesen, E. J. (1979). Performance of evaluation of computed tomography scanners using a phantom model. *American Journal of Roentgenology*, *132*, 345–352.

40. Goodenough, D. J., Weaver, K. E., & Davis, D. O. (1977). Development of a phantom for evaluation and assurance of image quality in ct scanning. *Optical Engineering*, *16*, 52–65.
41. Goodenough, D. J., Levy, J. R., & Kasales, C. (1998). Development of phantoms for spiral CT. *Comput Med Imag Grap*, *22*, 247–255.
42. White, D. R., Martin, R., & Darlison, R. (1977). Epoxy resin based tissue substitutes. *British Journal of Radiology*, *50*, 814–821.
43. The Phantom Laboratory. (2012b). Catphan[®] 500 and 600 manual. Available on line in <http://www.phantomlab.com/library/pdf/catphan500-600manual.pdf>.
44. The Institute of Physics and Engineering in Medicine. (1997). Recommended standards for the routine performance testing of diagnostic x-ray imaging systems. *IPEM Report No 77*. Institute of Physics and Engineering in Medicine, New York.
45. The Institute of Physics and Engineering in Medicine. (2003). Measurement of the performance characteristics of diagnostic x-ray systems used in medicine. *IPEM Report No: 32 Part III: Computed tomography x-ray scanners* (2nd edition). York, Institute of Physics and Engineering in Medicine.
46. European Commission. (2000). European guidelines on quality criteria for computed tomography. EUR 16262 EN. Luxembourg, Office for Official Publications of the European Communities.
47. American College of Radiology. (2012). CT accreditation program requirements. Available in <http://www.acr.org/~/media/ACR/Documents/Accreditation/CT/Requirements.pdf>.
48. McCollough, C. H., Bruesewitz, M. R., McNitt-Gray, M. F., Bush, K., Ruckdeschel, T., Payne, J. T., et al. (2004). The phantom portion of the American College of Radiology (ACR) computed tomography (CT) accreditation program: Practical tips, artifact examples, and pitfalls to avoid. *Medical Physics*, *31*, 2423–2442.
49. Alderson, S. W., Lanzl, L. H., Rollins, M., & Spira, J. (1962). An instrumented phantom system for analog computation of treatment plans. *American Journal of Roentgenology*, *87*, 185–195.
50. White, D. R. (1978). Tissue substitutes in experimental radiation physics. *Medical Physics*, *5*, 467–479.
51. Archer, B. R., Glaze, S., North, L. B., & Bushong, S. C. (1977). Dosimeter placement in the rando phantom. *Medical Physics*, *4*, 315–318.
52. Vacirca, S. J., Pasternack, B. S., & Blatz, H. (1972). A film-thermoluminescent dosimetry method for predicting body doses due to diagnostic radiography. *Physics in Medicine & Biology*, *17*, 71–80.
53. Yalcintas, M. G., & Nalcioğlu, O. (1979). A method for dose determination in computerized tomography. *Health Physics*, *37*, 543–548.
54. Fullerton, G. D., & White, D. R. (1979). Anthropomorphic test objects for CT scanners. *Radiology*, *133*, 217–222.
55. The Phantom Laboratory. (2012a). RAN 100 and RAN 110 datasheet brochure. Available on line in http://www.phantomlab.com/library/pdf/rando_datasheet.pdf.
56. Nikolic, B., Khosa, F., Lin, P. J. P., Khan, A. N., Sarwar, S., Yam, C.-S., et al. (2010). Absorbed radiation dose in radiosensitive organs during coronary CT angiography using 320-MDCT: Effect of maximum tube voltage and heart rate variations. *American Journal of Roentgenology*, *195*, 1347–1354.
57. Hurwitz, L. M., Yoshizumi, T. T., Reiman, R. E., Paulson, E. K., Frush, D. P., Nguyen, G. T., et al. (2006). Radiation dose to the female breast from 16-MDCT body protocols. *American Journal of Roentgenology*, *186*, 1718–1722.
58. Litmanovich, D., Tack, D., Lin, P. J., Boiselle, P. M., Raptopoulos, V., Bankier A. A., (2011). Female breast, lung, and pelvic organ radiation from dose-reduced 64-MDCT thoracic examination protocols: a phantom study. *AJR Am J Roentgenol*. 197(4), 929–934. doi: 10.2214/AJR.10.6401.
59. Deak, P., van Straten, M., Shrimpton, P. C., Zankl, M., & Kalender, W. A. (2008). Validation of a Monte Carlo tool for patient-specific dose simulations in multi-slice computed tomography. *European Radiology*, *18*, 759–772.

60. International Commission on Radiological Protection. (2007a). *The 2007 recommendations of the international commission on radiological protection*. ICRP Publication 103. Elsevier ed.
61. Huda, W., Atherton, J. V., Ware, D. E., & Cumming, W. A. (1997). An approach for the estimation of effective radiation dose at CT in pediatric patients. *Radiology*, 203, 417–422.
62. Deak, P. D., Smal, Y., & Kalender, W. A. (2010). Sex- and age-specific conversion factors used to determine effective dose from Dose-Length product. *Radiology*, 257, 158–166.
63. Cristy, M. (1980). Mathematical phantoms representing children of various ages for use in estimates of internal dose. Report no. ORNL/NUREG/TM-367. Oak Ridge, Tenn: Oak Ridge National Laboratory.
64. Melo Lima, V. J., Cassola, V. F., Kramer, R., de Oliveira Lira, C. A. B., Khoury, H. J., & Vieira, J. W. (2011). Development of 5- and 10-year-old pediatric phantoms based on polygon mesh surfaces. *Medical Physics*, 38, 4723–4736.
65. Kramer, R., Vieira, J. W., Khoury, H. J., Lima, F. R. A., & Fuelle, D. (2003). All about MAX: A male adult voxel phantom for Monte Carlo calculations in radiation protection dosimetry. *Physics in Medicine & Biology*, 48, 1239–1262.
66. Cassola, V. F., de Melo Lima, V. J., Kramer, R., & Khoury, H. J. (2010). FASH and MASH: Female and male adult human phantoms based on polygon mesh surfaces. Part I: Development of the anatomy. *Physics in Medicine & Biology*, 55, 133–162.
67. Kramer, R., Cassola, V. F., Vieira, J. W., Khoury, H. J., de Oliveira Lira, C. A. B., & Brown, K. R. (2012). Skeletal dosimetry based on CT images of trabecular bone: update and comparisons. *Physics in Medicine & Biology*, 57, 3995–4021.
68. Boone, J. M., Geraghty, E. M., Seibert, J. A., & Wootton-Gorges, S. L. (2003). Dose reduction in pediatric CT: A rational approach. *Radiology*, 228, 352–360.
69. Strauss, K. J., Goske, M. J., Frush, D. P., Butler, P. F., & Morrison, G. (2009). Image Gently vendor summit: Working together for better estimates of pediatric radiation dose from CT. *American Journal of Roentgenology*, 192, 1169–1175.
70. Cody, D. D., Moxley, D. M., Krugh, K. T., O’Daniel, J. C., Wagner, L. K., & Eftekhari, F. (2004). Strategies for formulating appropriate MDCT techniques when imaging the chest, abdomen, and pelvis in pediatric patients. *American Journal Roentgenology*, 182, 849–859.
71. Brisse, H. J., Robilliard, M., Savignoni, A., Pierrat, N., Gaboriaud, G., De Rycke, Y., et al. (2009). Assessment of organ absorbed doses and estimation of effective doses from pediatric anthropomorphic phantom measurements for multi-detector row CT with and without automatic exposure control. *Health Physics*, 97, 303–314.
72. Birnbaum, B. A., Hindman, N., Lee, J., & Babb, J. S. (2007). Multi-detector row CT attenuation measurements: Assessment of intra- and interscanner variability with an anthropomorphic body CT phantom. *Radiology*, 242, 109–119.
73. Birnbaum, B. A., Hindman, N., Lee, J., & Babb, J. S. (2007). Influence of multidetector CT reconstruction algorithm and scanner type in phantom model. *Radiology*, 244, 767–775.
74. Wagner, L. K., Lester, R. G., & Saldana, L. R. (1985). *Exposure of the pregnant patient to diagnostic radiations: a guide to medical management*. Philadelphia: Lippincott.
75. Wagner, L. K., Archer, B. R., & Zeck, O. F. (1986). Conceptus dose from state-of-the-art CT scanners. *Radiology*, 159, 787–792.
76. Osei, E. K., & Faulkner, K. (1999). Fetal doses from radiological examinations. *British Journal of Radiology*, 72, 773–780.
77. Osei, E. K., Darko, J. B., Faulkner, K., & Kotre, C. J. (2003). Software for the estimation of fetal radiation dose to patients and staff in diagnostic radiology. *Journal of Radiological Protection*, 23, 183–194.
78. Osei, E. K., & Faulkner, K. (2000). Radiation risks from exposure to diagnostic x-rays during pregnancy. *Radiography*, 6, 131–144.
79. Osei, E. K., & Barnett, R. (2009). Software for the estimation of organ equivalent and effective doses from diagnostic radiology procedures. *Journal of Radiological Protection*, 29, 361–376.

80. Osei, E. K., & Darko, J. (2013). A survey of organ equivalent and effective doses from diagnostic radiology procedures. *ISRN Radiology*, 2013, 1–9.
81. Felmlee, J. P., Gray, J. E., Leetzow, M. L., & Price, J. C. (1990). Estimated fetal radiation dose from multislice CT studies. *American Journal of Roentgenology*, 154, 185–190.
82. Dietrich, M. F., Miller, K. L., & King, S. H. (2005). Determination of potential uterine (conceptus) doses from axial and helical CT scans. *Health Physics*, 88, S10–S13.
83. Hurwitz, L. M., Yoshizumi, T., Reiman, R. E., Goodman, P. C., Paulson, E. K., Frush, D. P., et al. (2006). Radiation dose to the fetus from body MDCT during early gestation. *American Journal of Roentgenology*, 186, 871–876.
84. Jaffe, T. A., Neville, A. M., Anderson-Evans, C., Long, S., Lowry, C., Yoshizumi, T. T., et al. (2009). Early first trimester fetal dose estimation method in a multivendor study of 16- and 64-mdct scanners and low-dose imaging protocols. *American Journal of Roentgenology*, 193, 1019–1024.
85. Jaffe, T. A., Yoshizumi, T. T., Toncheva, G. I., Nguyen, G., Hurwitz, L. M., & Nelson, R. C. (2008). Early first-trimester fetal radiation dose estimation in 16-MDCT without and with automated tube current modulation. *American Journal of Roentgenology*, 190, 860–864.
86. Gilet, A. G., Dunkin, J. M., Fernandez, T. J., Button, T. M., & Budorick, N. E. (2011). Fetal radiation dose during gestation estimated on an anthropomorphic phantom for three generations of CT scanners. *American Journal of Roentgenology*, 196, 1133–1137.
87. Wang, J., Christner, J. A., Duan, X., Leng, S., Yu, L., & McCollough, C. H. (2012). Attenuation-based estimation of patient size for the purpose of size specific dose estimation in CT. Part II. Implementation on abdomen and thorax phantoms using cross sectional CT images and scanned projection radiograph images. *Medical Physics*, 39, 6678–6772.
88. Peng, G., Zeng, Y., Luo, T., Zhao, F., Peng, S., You, R., et al. (2012). Organ dose evaluation for multi-slice spiral ct scans based on China Sichuan chest anthropomorphic phantom measurements. *Radiation Protection Dosimetry*, 150, 292–297.
89. McCollough, C.H. (2011). Translating protocols across patient size: Babies to bariatric. Lecture in the 2011 AAPM Summit on CT Dose. October 7–8 2011, Denver, CO.
90. Duan, X., Wang, J., Christner, J. A., Leng, S., Grant, K. L., & McCollough, C. H. (2011). Dose reduction to anterior surfaces with organ-based tube-current modulation: Evaluation of performance in a phantom study. *American Journal of Roentgenology*, 197, 689–695.
91. Matsubara, K., Koshida, K., Ichikawa, K., Suzuki, M., Takata, T., Yamamoto, T., et al. (2009). Misoperation of CT automatic tube current modulation systems with inappropriate patient centering: Phantom studies. *American Journal of Roentgenology*, 192, 862–865.
92. Kalender, W. A., Wolf, H., & Suess, C. (1999). Dose reduction in CT by anatomically adapted tube current modulation. II. Phantom measurements. *Medical Physics*, 26, 2248–2253.
93. Keat, N. (2005). *CT scanner automatic exposure control system*. ImPACT report 05016. MHRA reports, London.
94. Flohr, T. G., Bruder, H., Stierstorfer, K., Petersilka, M., Schmidt, B., & McCollough, C. H. (2008). Image reconstruction and image quality evaluation for a dual source CT scanner. *Medical Physics*, 35, 5882–5897.
95. McCollough, C. H., Primak, A. N., Saba, O., Bruder, H., Stierstorfer, K., Raupach, R., et al. (2007). Dose performance of a 64-channel dual-source CT scanner. *Radiology*, 243, 775–784.
96. Capeleti, F.F., Melo, C.S., Furquim, T.A.C., Nersissian, D.Y. (2011). Phantom development for quality control in automatic exposure control in computed tomography systems. *Poster Presented on 18th International Conference of Medical Physics*, April 17–20 2011, Porto Alegre, Brazil.
97. Morehouse, C. C., Brody, W. R., Guthaner, D. F., Breiman, R. S., & Harell, G. S. (1980). Gated cardiac computed tomography with a motion phantom. *Radiology*, 134, 213–217.
98. Boll, D. T., Merkle, E. M., Paulson, E. K., & Fleiter, T. R. (2008). Dual-Energy multidetector CT assessment in a pilot study with anthropomorphic phantom. *Radiology*, 247, 687–695.

99. Driscoll, B., Coolens, C., & Keller, H. (2011). Quantitative DCE-CT imaging quality assurance with a novel dynamic flow phantom. *Medical Physics*, *38*, 3874.
100. Horiguchi, J., Kiguchi, M., Fujioka, C., Shen, Y., Arie, R., Sunasaka, K., et al. (2008). Radiation dose, image quality, stenosis measurement, and CT densitometry using ECG-Triggered coronary 64-MDCT angiography: A phantom study. *American Journal of Roentgenology*, *190*, 315–320.
101. Nosratiéh, A., Yang, K., Aminololama-Shakeri, S., & Boone, J. M. (2012). Comprehensive assessment of the slice sensitivity profiles in breast tomosynthesis and breast CT. *Medical Physics*, *39*, 7254–7261.
102. Szegedi, M., Szegedi, P. R., Sarkar, V., Hinkle, J., Wang, B., Huang, Y., et al. (2012). Tissue characterization using a phantom to validate four-dimensional tissue deformation. *Medical Physics*, *39*, 6065–6070.
103. McNitt-Gray, M. (2013). CT dose measurements. Lecture presented at Hands-on Workshop for Physicists. MD Anderson Cancer Center, February 8–10, 2013.